

MIT Open Access Articles

Development of a gamma-ray detector with iridium transition edge sensor coupled to a Pb absorber

The MIT Faculty has made this article openly available. **Please share** how this access benefits you. Your story matters.

Citation: Damayanthi, R. et al. "Development of a Gamma-Ray Detector With Iridium Transition Edge Sensor Coupled to a Pb Absorber." Applied Superconductivity, IEEE Transactions on 19.3 (2009): 540-543. © 2009, IEEE

As Published: <http://dx.doi.org/10.1109/TASC.2009.2019295>

Publisher: Institute of Electrical and Electronics Engineers

Persistent URL: <http://hdl.handle.net/1721.1/59849>

Version: Final published version: final published article, as it appeared in a journal, conference proceedings, or other formally published context

Terms of Use: Article is made available in accordance with the publisher's policy and may be subject to US copyright law. Please refer to the publisher's site for terms of use.



Development of a Gamma-Ray Detector With Iridium Transition Edge Sensor Coupled to a Pb Absorber

Rathnayaka Mudiyansele Thushara Damayanthi, Steven W. Leman, Hiroyuki Takahashi, Masashi Ohno, Yasuhiro Minamikawa, Kentaro Nishimura, and Naoko Iyomoto

Abstract—We have recently started to develop a high-resolution gamma-ray spectrometer for material defect analysis. Our gamma-ray detector is a microcalorimeter consisting of an iridium/gold bilayer transition edge sensor (TES) thermometer and a bulk Pb absorber, which is directly coupled to a TES with Stycast 2850FT epoxy. This paper describes our TES based gamma-ray detector and the first experimental results for 662 keV and 1173 keV incident gamma-rays. We report an energy resolution of 4.7 keV at 662 keV and 2.9 keV at 1173 keV.

Index Terms—Bulk Pb absorber, gamma-ray spectroscopy, iridium, transition-edge sensors.

I. INTRODUCTION

GAMMA-RAY spectroscopy is an important technique in the nondestructive assay of nuclear materials. We are developing a high-resolution gamma-ray spectrometer to measure high-energy gamma-rays for Coincidence Doppler Broadening (CDB) Positron Annihilation Spectroscopy (PAS) studies [1]. PAS analysis can be applied to study damage to nuclear reactor pressure vessels (RPV), which results from neutron irradiation during reactor operation. A high energy resolution detector is necessary to distinguish between the metal RPV's Fermi (resulting from voids/damage in the RPV) and bound electron momentum distributions. The energy resolution of commercially available high purity germanium (HPGe) detectors is limited by the Fano statistics of electrons that are produced in the absorber bulk and is limited to ~ 1 keV full width at half maximum (FWHM) at 511 keV. Transition Edge Sensor (TES) based gamma-ray detectors do not suffer from this limitation and a resolution of 25 eV at 103 keV has been reported with a

Manuscript received August 25, 2008. First published June 30, 2009; current version published July 10, 2009. This work was supported in part by a Grant-in-Aid for research 656288 (2004) from the Ministry of Education, Culture, Sports, Science and Technology, Japan.

R. M. T. Damayanthi, H. Takahashi, Y. Minamikawa, K. Nishimura, and N. Iyomoto are with the Department of Nuclear Engineering and Management, the University of Tokyo, 7-3-1, Hongo, Bunkyo-ku, Tokyo, 113-8656 Japan (e-mail: thushara@sophie.q.t.u-tokyo.ac.jp; leo@n.t.u-tokyo.ac.jp; minami@sophie.q.t.u-tokyo.ac.jp; ken@sophie.q.t.u-tokyo.ac.jp; iyomoto@nuclear.jp).

M. Ohno is with the Department of Nuclear Engineering and Management, the University of Tokyo, 7-3-1, Hongo, Bunkyo-ku, Tokyo, 113-8656 Japan. He is also with PRESTO, Japan Science and Technology Agency (e-mail: ohno@n.t.u-tokyo.ac.jp).

S. W. Leman was with the University of Tokyo, Japan. He is now with the Kavli Institute for Astrophysics and Space Research, Massachusetts Institute of Technology, Cambridge MA 02139, USA (e-mail: swleman@MIT.EDU).

Color versions of one or more of the figures in this paper are available online at <http://ieeexplore.ieee.org>.

Digital Object Identifier 10.1109/TASC.2009.2019295

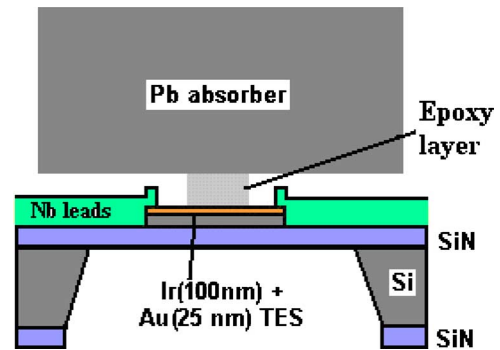


Fig. 1. The cross sectional view of the composite gamma-ray detector.

Mo/Cu bilayer TES with an epoxy coupled tin (Sn) absorber [2]. Although TES based gamma-ray detectors have been studied by various research groups they have previously only been studied up to energies of ~ 100 keV [2]–[4].

In this paper we present experiment results obtained with our first TES based gamma-ray detector, measured for high-energy gamma-rays. Our detector incorporates a lead (Pb) absorber; an absorber type which has not been previously reported on. We determine a FWHM energy resolution of 4.7 keV at 662 keV (0.7%), and 2.9 keV at 1173 keV (0.2%). We plan to optimize a future device to improve energy resolution.

II. DETECTOR DESIGN AND EXPERIMENTAL SETUP

A microcalorimeter consists of three main parts, an absorber to stop incident photons, a thermometer that measures the temperature increase of the absorber, and a weak thermal link to a cold bath that returns the absorber temperature to some defined value in the absence of incident radiation.

A cross sectional view of our composite gamma-ray detector is shown in Fig. 1. The detector is comprised of a TES thermometer, which operates in the narrow transition region between the superconducting and normal states. A small change of temperature (~ 1 mK) causes a large change of resistance ($\sim 1 \Omega$) making a very sensitive thermometer. Our TES thermometer is an iridium/gold bilayer device with niobium electrical leads. The Ir/Au bilayer film is $200 \mu\text{m} \times 200 \mu\text{m}$. The thicknesses of the Ir and Au films are 100 nm and 25 nm respectively.

The Pb absorber is the largest part of this detector. Photoelectric absorption cross section of a material, σ_{pe} , is roughly expressed by

$$\sigma_{pe} \propto \frac{Z^n}{E_\gamma^{3.5}}, \quad (1)$$

where Z is the atomic number, E_{Γ} is the energy of an incident gamma-ray photon, and n varies between 4 and 5. Since photoelectric absorption is the preferred mode of interaction, absorber materials of high Z are preferable for gamma-ray detectors. While the material should be thick enough to stop incident photons, it should have a small heat capacity to increase the temperature sensitivity. Elemental superconductors satisfy these requirements. Tin (Sn) is used for detectors developed in the ~ 100 keV range [2]–[4]. However, in the high energy range, Pb's high Z provides two benefits compared to Sn. First, 662 keV gamma-rays have a 0.85 cm attenuation length in Pb compared to 1.88 cm in Sn [5]. Second, for energies greater than a few hundred keV, Compton scattering dominates over photoelectric absorption. At 662 keV, Pb's Compton scattering to photoelectric cross section ratio is ~ 1.4 and is favorably higher than Sn's ratio of 7.8.

The low absorption efficiency for high-energy gamma-rays poses a challenge in gamma-ray spectroscopy. Absorption efficiency improves with thicker absorbers but at the cost of increased heat capacity. A small heat capacity device is required for high-resolution gamma-ray spectrometers, because energy resolution of microcalorimeters goes as, $\Delta E_{FWHM} \propto \sqrt{C}$, where C is the heat capacity of the device. To provide a balance between these constraints, our Pb absorber is 1 mm \times 1 mm \times 0.75 mm. The photoelectric absorption efficiency is 100% at ~ 100 keV, but is reduced at higher energies to $\sim 8.5\%$ at 662 keV and 5% at 1173 keV. The heat capacity of our composite detector is dominated by the absorber with a total value of 71 pJ/K.

The Pb absorber and TES are thermally well coupled by a 0.0004 cm² area, ~ 50 μ m thick Stycast epoxy layer. The thermal conductivity of the Stycast epoxy layer is calculated by,

$$G_{Sty} = A \times T^B \frac{Area_{Sty}}{Length_{Sty}}, \quad (2)$$

where A and B are material related constants and for Stycast 2850FT, $A = 92$ μ W/cmK and $B = 2.65$ [6]. The thermal conductance of the epoxy layer is ~ 16 nW/K. The TES and cold bath are weakly coupled through a 400 nm thick silicon nitride (SiN) membrane having a 310 pW/K thermal conductance.

For testing, the gamma-ray detector was mounted on the cold stage (64 mK) of a ³He/⁴He dilution refrigerator. The TES is voltage biased with a 3 m Ω shunt resistance, allowing negative electrothermal feedback (ETF) to maintain the TES at $0.4R_n$, where R_n is the normal resistance of the device [7]. Our iridium/gold bilayer TES devices have a transition temperature, $T_c \sim 110$ mK. However, after attaching the absorber with Stycast the T_c dropped to ~ 95 mK and the shape of the superconducting transition was considerably distorted, and effect that may be due to the stress of epoxy layer. This kind of effect has been reported upon before [8].

The detector was irradiated separately by two gamma-ray sources, which were located outside of the cryostat. The ¹³⁷Cs source produced 662 keV gamma-rays and the ⁶⁰Co source produced 1173 keV and 1332 keV gamma-rays.

Incident gamma-rays heat the absorber leading to an increase in resistance, and corresponding decreasing in current flowing through the TES. This current decrease is amplified by a 200 series arrayed superconducting quantum interference device

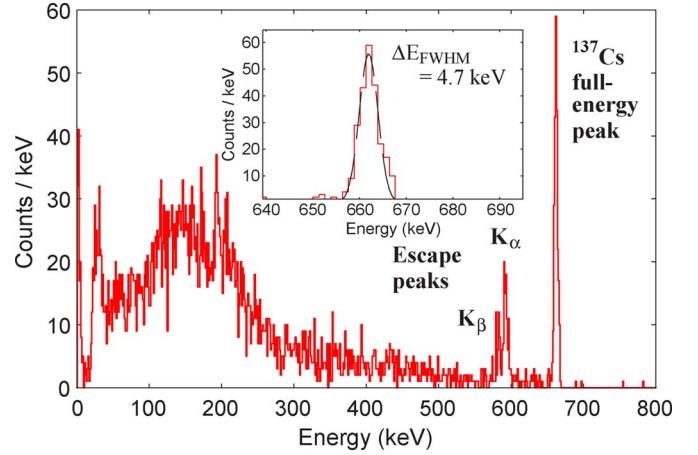


Fig. 2. Energy spectrum recorded from 662 keV gamma-rays emitted by a ¹³⁷Cs source showing the photoelectron absorption peak and Pb K_{α} and K_{β} escape peaks (75 keV and 85 keV below the photopeak). The Compton continuum is complicated by various energy escape processes. Inset is the enlarge view of 662 keV photoelectron peak with its Gaussian fit (dashed line) of 4.7 keV FWHM energy resolution.

(SQUID) current amplifier [9]. The signal is digitizer sampled at 50 kHz and recorded using LabVIEW programs. Finally, the traces are analysed using an optimal filter technique [10].

III. EXPERIMENTAL RESULTS

A. ¹³⁷Cs Gamma-Ray Spectrum

We illuminated the detector with a ¹³⁷Cs source that supplied mono-energetic 662 keV gamma-rays at a rate of 0.4 cps. Because the ratio of the Compton to photoelectric cross section is large, a greater fraction of all detected events lied within the Compton continuum (95%) rather than under the photopeak (5%). Fig. 2 shows the 662 keV photoelectron peak of ¹³⁷Cs with a full width at half maximum (FWHM) energy resolution of 4.7 keV (0.7%) and the Pb K_{α} and K_{β} X-ray escape peaks (75 and 85 keV below the photopeak) are indicated in the figure.

At very low energies (< 100 keV) the Compton continuum may effectively disappear. But for high-energy ¹³⁷Cs gamma-rays the most prominent part is the Compton continuum. In our spectrum the ~ 477 keV Compton edge is not clearly resolvable. The possibility of multiple Compton scattering followed by escape of the final scattered photon can lead to a total energy deposition that is greater than the calculated value of the Compton edge. These multiple events can thus partially fill in the gap between the Compton edge and the photoelectron peak, as well as distort the shape of the continuum. In addition, secondary electron escape and effects of surrounding materials complicate the spectrum. All preceding effects contributed to result in a complicated spectrum for 662 keV gamma-rays.

Position dependence in the large absorber might degrade the energy resolution, since thermal diffusion inside the absorber causes a fluctuation of pulse shape. Also the slow response of our detector limits the counting rate. In the next section we will discuss the signal response and how to improve the counting rate. However, we believe the energy resolution degradation is dominated by the detector's large base line noise of 1.56 keV

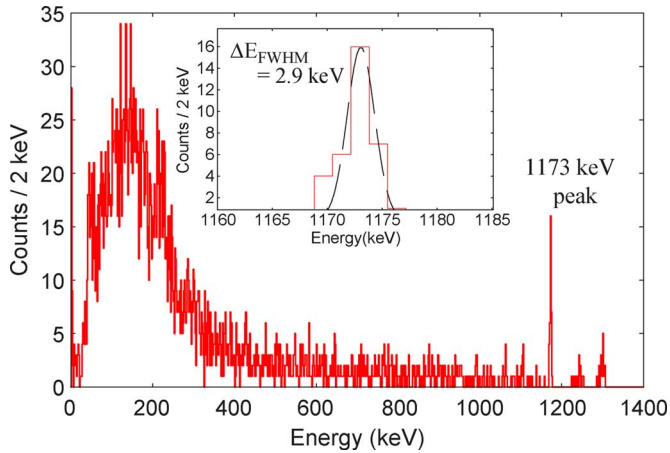


Fig. 3. Energy spectra recorded with a ^{60}Co source indicating 1173 keV photoelectric absorption peak. 1332 keV peak is not sharp due to the saturation of current pulses at this energy. Inset is the enlarged view of 1173 keV photoelectron peak with its Gaussian fitting line (dashed line) of 2.9 keV FWHM energy resolution.

(measured). Additionally, we observed a periodic fluctuation of the base line, affected by the temperature fluctuations of the cryostat and mechanical vibrations of the rotary pump.

B. ^{60}Co Gamma-Ray Spectrum

As an additional characterization, we illuminated the detector with a ^{60}Co source that simultaneously supplied both 1173 keV and 1332 keV gamma-rays at a rate of 0.35 cps. We observed 0.9% and 0.6% of the events in the 1173 keV and 1332 keV photopeaks respectively, with the remainder of the events contained in the Compton continuum.

Fig. 3 shows the energy spectra of ^{60}Co showing the Compton continuum and photoelectron peaks. However, as explained in the next section, the signal is saturated for the 1332 keV gamma-rays. Therefore the 1332 keV peak is not sharp when we applied optimal filtering. The inset shows a clear view of 1173 keV photoelectron peak with its fitting line and we estimated a FWHM energy resolution of 2.9 keV (0.2%) at 1173 keV.

C. Current Response

Fig. 4(a) shows the measured current responses to 662 keV, 1173 keV and 1332 keV gamma-rays. We observe that the signal has saturated for 1332 keV gamma-ray photons.

Current pulses have a $\sim 150 \mu\text{s}$ rise time (10%–90%) and a 140 ms fall time. From material properties we have calculated a much shorter C/G decay time of 1.7 ms, which is limited by coupling between the absorber and the TES. We fitted the current pulse of ^{137}Cs with a formula,

$$f(x) = a \times \exp[-(x - b)/c] \quad (3)$$

where a is the pulse height, b is the time origin of the current pulse and c is the decay time constant. The decay curve could be fitted with two distinct exponential decay curves, a fast component followed by a very slow component as shown in the Fig. 4(b). However, there is an ambiguous part in between these

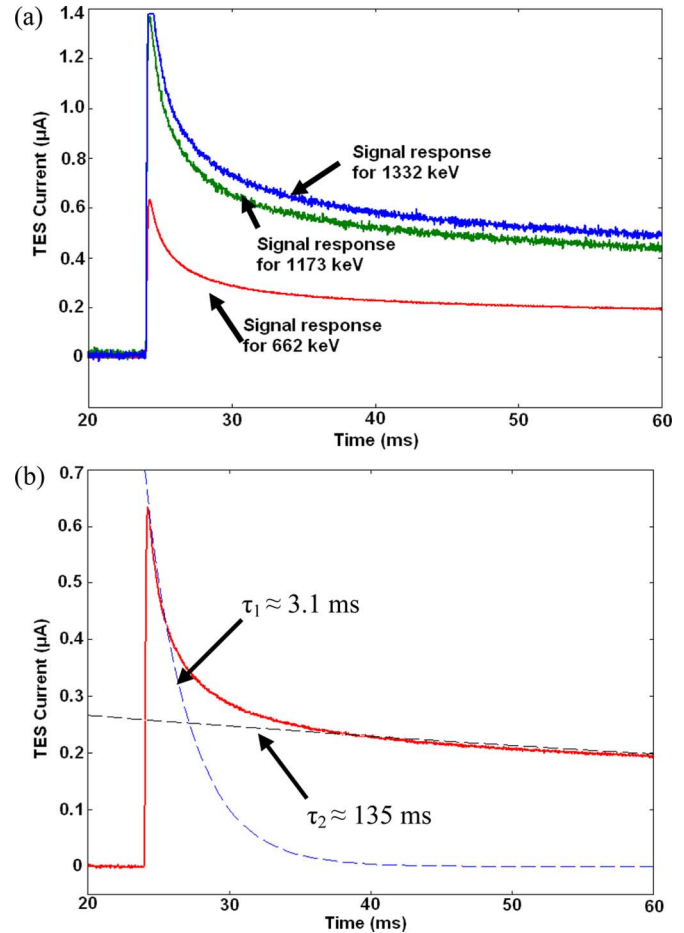


Fig. 4. (a) Measured signal pulse responses of the TES based gamma detector to 662 keV, 1173 keV and 1332 keV gamma-rays. Rise time and fall time of response curves are $\sim 150 \mu\text{s}$ and $\sim 140 \text{ms}$ respectively. Pulse has saturated for 1332 keV gamma-rays. (b) Response curve for ^{137}Cs with its two distinct decay time constants, fast component of 3.1 ms followed by a slow component of $\sim 135 \text{ms}$. There is an ambiguous part in between them, which can not be fit with exponential fitting formula.

two components, which can not be fit with this method. The best fit values of the fast and slow components are 3.1 ms and 135 ms respectively. The fast time constant corresponds to the time constant of energy flowing out of the absorber through the epoxy, given by $C_{\text{abs}}/G_{\text{epoxy}} \approx 4 \text{ms}$. The mismatch is due to the uncertainty of thickness of epoxy layer.

The $C_{\text{abs}}/G_{\text{epoxy}}$ time constant limits the thermal decay time constant. Since large area absorbers are required to increase the count rate and collecting area, the most effective way to reduce the decay time is by increasing the thermal conductivity between the absorber and TES. The largest uncertainty of our detector geometry is the Stycast epoxy layer. In this device fabrication, the epoxy application was not well controlled. By controlling the amount of epoxy, the decay time could be shorter. In our new device we plan to fabricate a stem on the TES and post the absorber on it to control the amount of epoxy.

The thermal conductivity between the Pb absorber and TES will be improved in our next device by reducing the epoxy layer thickness. Also we should make efforts to minimize the second time constant to improve the count rate and energy resolution of our detector.

Although the long time constant is not yet understood we think it is due to an athermal time constant seen in other superconducting absorbers [11]. A likely possibility for an athermal response may be long-lived quasiparticles. Pb's Debye temperature and superconducting gap are close in energy and may allow for resonances between the phonon and quasiparticle systems leading to these long-lived quasiparticles. The long recovery time of athermal phonons limits the counting rate of the detector. Since there are not any reported results for Pb absorbers we intend to carefully study the physics of the Pb absorber to clarify and to understand the source of the long athermal time constant.

IV. CONCLUSION

Our first detector has confirmed that a TES based gamma-ray detector is applicable to high-energy gamma-ray spectroscopy. We report an energy resolution of 4.7 keV at 662 keV and 2.9 keV at 1173 keV.

In our next device we will optimize the detector heat capacity, and thermal coupling between the Pb absorber and TES. We are beginning studies of the Pb absorber physics to reduce of athermal time constants.

ACKNOWLEDGMENT

Transition edge sensor devices were fabricated at the VLSI design and education center (VDEC), The University of Tokyo.

REFERENCES

[1] S. W. Leman and H. Takahashi, "Development of transition edge sensor gamma-ray detectors for positron-annihilation-spectroscopy," *J Low Temp. Phys.*, vol. 151, pp. 784–789, 2008.

[2] W. B. Doriese, J. N. Ullom, J. A. Beall, W. D. Duncan, L. Ferreira, G. C. Hilton, R. D. Horansky, K. D. Irwin, J. A. B. Mates, C. D. Reintsema, L. R. Vale, Y. Xu, and B. L. Zink, "14-pixel, multiplexed array of gamma-ray microcalorimeters with 47 eV energy resolution at 103 keV," *Appl. Phys. Lett.*, vol. 90, p. 193508, 2007.

[3] D. T. Chow, M. A. Lindeman, M. F. Cunningham, M. Frank, T. W. Barbee, Jr., and S. E. Labov, "Gamma-ray spectrometers using a bulk Sn absorber coupled to a Mo/Cu multilayer superconducting transition edge sensor," *Nucl. Instrum. Methods Phys. Res. A*, vol. 444, pp. 196–200, 2000.

[4] T. Oshima, Y. Yamakawa, H. Kurabayashi, A. Hoshina, T. Ohashi, K. Mitsuda, and K. Tanaka, "A high energy resolution gamma-ray TES microcalorimeter with fast response time," *J Low Temp. Phys.*, vol. 151, pp. 430–435, 2008.

[5] [Online]. Available: <http://physics.nist.gov/PhysRefData/Xcom/Text/XCOM.html>

[6] J. R. Olson, "Thermal conductivity of some common cryostat materials between 0.05 and 2 K," *Cryogenics*, vol. 33, no. 7, pp. 729–731, 1993.

[7] K. D. Irwin, G. C. Hilton, D. A. Wollman, and J. M. Martinis, "X-ray detection using a superconducting transition-edge sensor microcalorimeter with electrothermal feedback," *Appl. Phys. Lett.*, vol. 69, pp. 1945–1947, 1996.

[8] W. B. Doriese, J. N. Ullom, J. A. Beall, W. D. Duncan, L. Ferreira, G. C. Hilton, R. D. Horansky, K. D. Irwin, J. A. B. Mates, C. D. Reintsema, D. R. Schmidt, L. R. Vale, Y. Xu, B. L. Zink, M. K. Bacrania, A. S. Hoover, C. R. Rudy, M. W. Rabin, C. A. Kilbourne, K. R. Boyce, L. E. Brown, J. M. King, and F. S. Porter, "Toward a 256-pixel array of gamma-ray microcalorimeters for nuclear-materials analysis," *J Low Temp. Phys.*, vol. 151, pp. 754–759, 2008.

[9] F. Hirayama, N. Kasai, and M. Koyanagi, "Design of series SQUID array suppressing Josephson oscillation interference between element SQUIDs," *IEEE Trans. Appl. Super.*, vol. 9, no. 2, pp. 2923–2926, 1999.

[10] E. Figueroa-Feliciano, B. Cabrera, A. J. Miller, S. F. Powell, T. Saab, and A. B. C. Walker, "Optimal filter analysis of energy-dependent pulse shapes and its application to TES detectors," *Nucl. Instrum. Methods Phys. Res. A*, vol. 444, pp. 453–456, 2000.

[11] R. D. Horansky, J. N. Ullom, J. A. Beall, W. B. Doriese, W. D. Duncan, L. Ferreira, G. C. Hilton, K. D. Irwin, C. D. Reintsema, L. R. Vale, B. L. Zink, A. Hoover, C. R. Rudy, D. M. Tournear, D. T. Vo, and M. W. Rabin, "Superconducting absorbers for use in ultra-high resolution gamma-ray spectrometers based on low temperature microcalorimeter arrays," *Nucl. Instrum. Methods Phys. Res. A*, vol. 579, no. 1, pp. 169–172, 2007.